11TH INTERNATIONAL SYMPOSIUM ON FLOW VISUALIZATION
August 9-12, 2004, University of Notre Dame, Notre Dame, Indiana, USA

A RESONANT PULSE DETONATION ACTUATOR FOR HIGH-SPEED BOUNDARY LAYER SEPARATION CONTROL

B. T. Beck*, A. D. Cutler , J. P. Drummond***, S. B. Jones******

*** Kansas State University, Department of Mechanical & Nuclear Engineering
302 Rathbone Hall, Manhattan, KS 66506 USA, Email: tbeck@ksu.edu**

**** The George Washington University, 303 Butler Farm Road, Suite 106A
Hampton, VA 23666, Email: adcutler@gwu.edu**

***** NASA Langley Research Center, Mail Stop 197, Hypersonic Airbreathing Propulsion Branch, Aerodynamics, Aerothermodynamics, and Acoustics Competency, Hampton VA 23681-2199 USA, Email: j.p.drummond@nasa.gov**

****** NASA Langley Research Center, Mail Stop 236, Advanced Sensing and Optical Measurement Branch, Aerodynamics, Aerothermodynamics, and Acoustics Competency, Hampton VA 23681-2199 USA, Email: stephen.b.jones@nasa.gov**

Keywords: *Schlieren, combustion, detonation, actuator*

ABSTRACT

A variety of different types of actuators have been previously investigated as flow control devices. Potential applications include the control of boundary layer separation in external flows, as well as jet engine inlet and diffuser flow control. The operating principles for such devices are typically based on either mechanical deflection of control surfaces (which include MEMS flap devices), mass injection (which includes combustion driven jet actuators), or through the use of synthetic jets (diaphragm devices which produce a pulsating jet with no net mass flow).

This paper introduces some of the initial flow visualization work related to the development of a relatively new type of combustion-driven jet actuator that has been proposed based on a pulse-detonation principle. The device is designed to utilize localized detonation of a premixed fuel (Hydrogen)-air mixture to periodically inject a jet of gas transversely into the primary flow. Initial testing with airflow successfully demonstrated resonant conditions within the range of acoustic frequencies expected for the design. Schlieren visualization of the pulsating air jet structure revealed axially symmetric vortex flow, along with the formation of shocks. Flow visualization of the first successful sustained oscillation condition is also demonstrated for one configuration of the current test section. Future testing will explore in more detail the onset of resonant combustion and the approach to conditions of sustained resonant detonation.

1 INTRODUCTION

1.1 Background

Boundary layer control can be broadly classified into passive and active control [1]. Common applications include the control of boundary layer separation in external flows to maintain the effectiveness of flaps and other control surfaces, and internal flow boundary layer control associated with the operation of jet engine inlet and diffuser flows. Passive control includes the use of common devices such as vortex generator tabs [2] to delay the onset of separation associated with ailerons. Active control includes the many leading and trailing edge devices used in conjunction with flow control over wing surfaces [3].

Actuators of various types play an important role in active boundary layer control. A variety of different actuator devices have previously been investigated as flow control devices for both internal and external boundary layer applications. The operating principles for such devices are typically based on either mechanical deflection, mass injection, or through the use of synthetic jets [4]. Mechanical actuator devices include conventional flap controls, as well as more recent MEMS flap devices. Mass injection actuators are those through which a net mass flow takes place, and include combustion driven jet actuators [5]. Synthetic jets are diaphragm devices that produce a pulsating jet for control of the boundary layer with no net mass flow injection [6]. A key parameter controlling the effectiveness of pulsating actuator devices in boundary layer control is the dimensionless pulsation frequency, F^+ [1]. Flow control utilizing pulsating or synthetic jets requires F+ ~ 1 or higher. For high-speed flows, this translates into the need for high frequencies in the kilohertz range, which is difficult to achieve.

1.2 Resonant Detonation Actuator

Combustion jet actuators offer the promise of increased effectiveness in supersonic flows due to their utilization of the highly energetic combustion process. One such device that has recently been investigated [1,5] is based on a deflagration (or subsonic wave) combustion process, in contrast to detonation where combustion waves characteristically propagate at supersonics speeds [7].

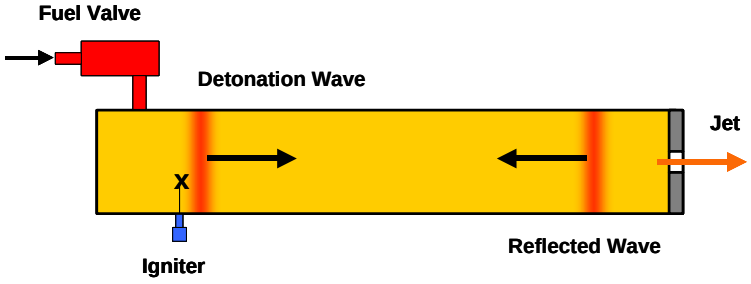

Figure 1: Resonant Detonation Actuator

A new type of combustion-driven jet actuator has been proposed based on a resonant pulse-detonation principle. This type device would potentially utilize internal resonance and localized detonation of a premixed fuel (Hydrogen-Air) mixture to periodically inject a jet of gas transversely into the primary flow. The intent is to produce a significantly more energetic jet interaction flow field than can be produced either with current zero-net-mass flux synthetic jet actuators, or with combustion mass injection utilizing only deflagration combustion. A simplified schematic of the basic actuator device currently under investigation is shown in Figure 1. It consists of an inlet valve

to control injection of fuel and air, some form of igniter to initiate combustion, a combustion chamber in which to develop the resonant combustion (detonation) phenomena, and a nozzle to both reflect the detonation wave as well as produce the desired exit pulsating high energy jet. An aspect of the proposed device as significant, and perhaps even more so than achieving detonation, is that it is designed to produce an internal longitudinal resonant oscillation condition within the combustion chamber. Achieving strong resonant wave motion within the combustion chamber is perhaps more important than achieving combustion, which has not yet been achieved in such a device. In principle, if a sufficiently strong resonant condition can be achieved, it would be possible to produce combustion without the need for periodic active (e.g., spark) ignition. With this type of sustained resonance, the potential also exists for operation of such a device without the need for moving parts to control the intake of fuel. The pressure oscillations associated with the combustion process would also be able to control the fuel intake.

Such an approach, if successful, should extend the effectiveness of actuator jet interaction for separation control well into the supersonic flow regime. The objectives here are to present initial work toward the development of a resonant detonation actuator utilizing hydrogen-air combustion. This paper presents the results of initial testing of one such actuator using airflow, which has successfully demonstrated resonant conditions within the range of acoustic frequencies expected for the design. Phase-locked Schlieren flow visualization images of the exit jet are presented, along with measurements of the associated periodic pressure oscillations within the "combustion chamber." Preliminary test results with actual combustion are also presented for one type of ignition sequence, which demonstrate the presence of sustained internal pressure oscillations.

2 EXPERIMENTAL FACILITY

2.1 Modular Actuator Test Section

A simplified orthographic view of the actual detonation actuator device tested in this paper is shown in Figure 2(a), and an actual photograph of one configuration of the actuator is shown in Figure 2(b). The actuator is designed to be modular, to allow investigation of different inlet fuel-air port location, as well as different combustion chamber lengths. It consists of a high-speed motor driven mixing valve assembly, a modular combustion chamber, and an end cap that forms the exit nozzle.

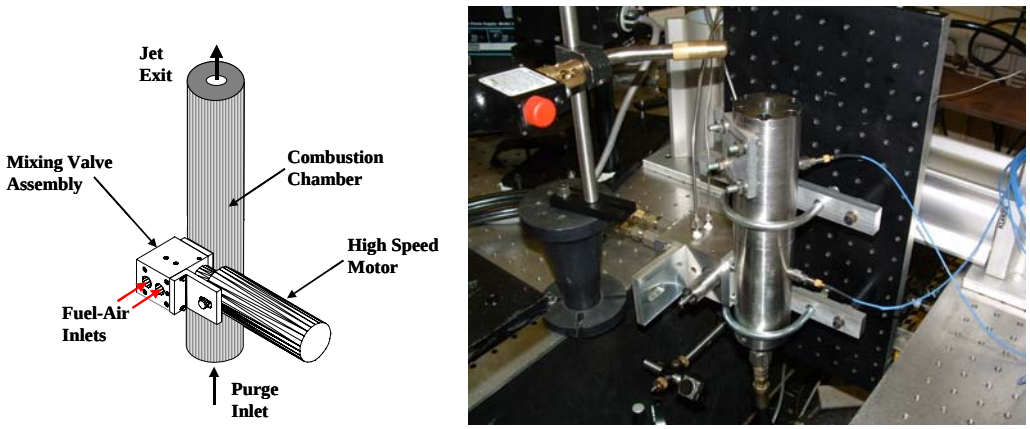

(a) Schematic Diagram of Actuator **(b) Photograph of Mounted Actuator Assembly**

Figure 2: Detonation Actuator Module

The combustion chamber is a modular design consisting of multiple cylindrical sections with an I.D. of 1.50 inches, an O.D. of 2.34 inches, and a length of 4.00 inches. The combustion chamber, as well as all other components, is uncooled; thus, only short-duration (5–10 s) combustion experiments were possible, followed by a cool down sequence using blown air. The sections have threaded ends consisting of male and female 1.5 inch straight pipe threads machined into each end for mating to adjacent sections. Buna-N O-rings were used to seal adjacent sections. Two combustion chamber sections are shown assembled in Figure 2(b). The base end cap is designed to provide a steady purge of inlet air for periodical flushing out the combustion products. The upper end cap is a straight bore nozzle with diameter 0.625 inches. The resonant actuator assembly is machined primarily from type 304 stainless steel. The end cap with the nozzle bore was attached to the adjacent section of the combustion chamber using six ¼-20 flat head machine screws, to provide a flush view of the exit plane of the jet. The end cap with purge inlet was mated to the end of the bottom section of the combustion chamber with 1.50 inch straight pipe thread and sealed with an O-ring.

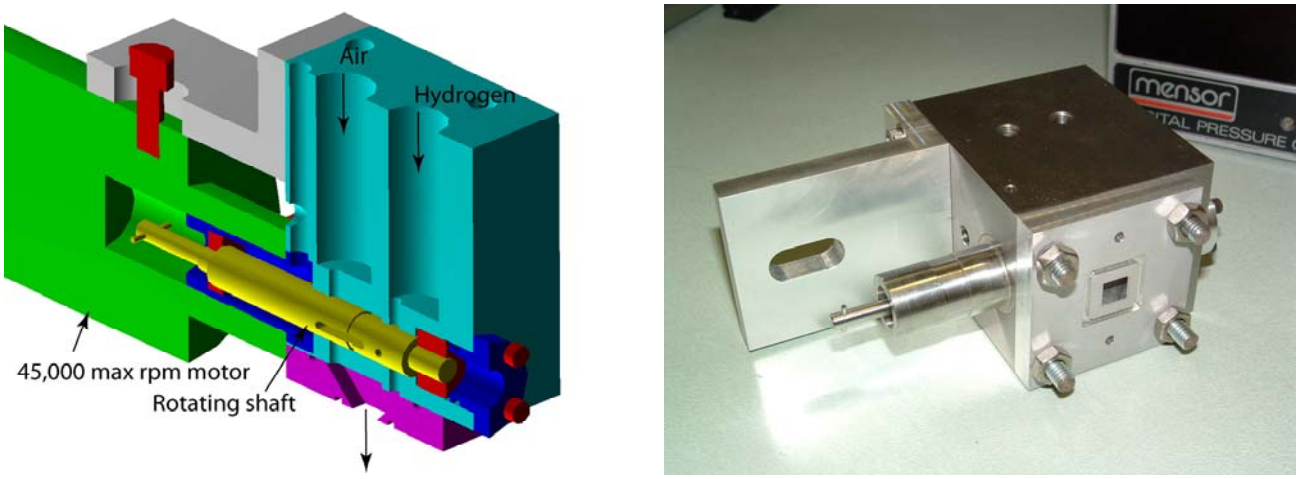

(a) Cross-sectional View of Mixing Valve **(b) Photograph of Mixing Valve Assembly**

Figure 3: Actuator Mixing Valve Assembly

A schematic drawing of the mixing valve assembly is shown in Figure 3(a) and an actual photograph is shown in Figure 3(b). The mixing valve assembly consists of a rotating shaft inlet porting system, which is designed to provide near stoichiometric mixture of Hydrogen and Air when the inlet pressures are equal. Tapered 1/8-inch pipe thread taps are provided for monitoring both inlet Hydrogen and inlet Air pressures. Except for the rotating shaft, which is machined from high-speed steel (15-5 H1025 stainless steel), the mixing valve is also machined from type 304 stainless steel.

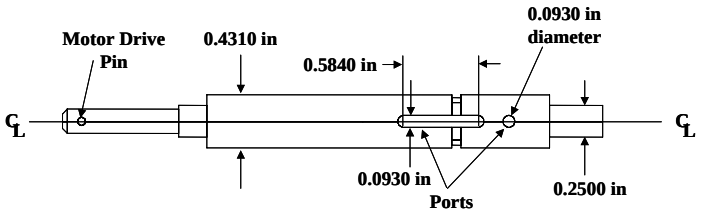

Figure 4: Rotating Shaft Porting System

Figure 4 shows the basic detail of the rotating shaft porting system. The slot shown ports the inlet air and the borehole, of diameter equal to the slot width, is designed for porting of the gaseous fuel (Hydrogen). The two gases are combined in the mixing valve assembly prior to entering the combustion chamber.

2.2 Actuator Flow Setup

A simplified schematic of the test setup used for the initial testing of the pulse detonation actuator device is shown in Figure 5. Pressurized air and gaseous hydrogen fuel in general were supplied separately to the actuator through the mixing valve inlet ports. For the initial tests, air only was

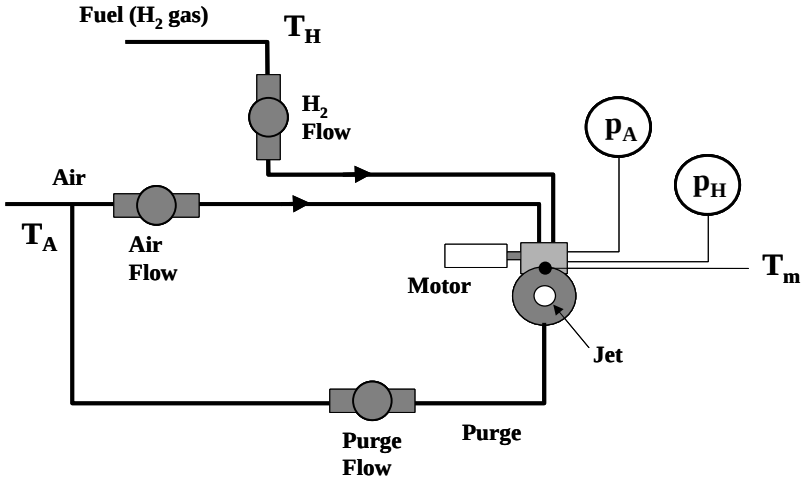

Figure 5: Air and Hydrogen Flow Setup

supplied to both fuel and air inlet ports, as well as to the purge port. Flow of air into the main air supply port was measured using a 0-2500 SLPM Hastings mass flow meter, the flow of air into the other (fuel) port was measured using a 0-1000 SLPM Hastings mass flow meter, and the purge air flow was measured using a 0-500 SLPM Hastings mass flow meter. Two pressure taps on the outside of the actuator mixing module allowed for individual pressure measurements of the fuel and air pressures within the module. For the initial air testing, the airflow into each inlet port was adjusted so as to approximately balance the two inlet pressures. In addition to the mixing chamber pressure measurements, pressures were also measured within the combustion chamber. Figure 2(b) shows the location of two such taps associated with this two-section 8-inch long combustion chamber configuration. The pressure sensors for the air tests were high frequency response 0-250 psi PCB sensors (Model 113A21) and a 3-channel Piezotronics signal conditioning unit model 480A21.

2.3 Flow Visualization Optical Setup

2.3.1 Schlieren Optical Setup

A Schlieren optical setup was used to provide flow visualization of the actuator exit jet, as shown in Figure 6. The setup was a standard Z-Type 2-mirror Schlieren system [8] consisting of a pulsed white light source, concave mirror pair, knife edge (razor blade), and image recording CCD camera.

Phase-delayed triggering of the light pulse was accomplished by using the trigger output from a digital oscilloscope, as shown. This provided phase-locked images of the periodic jet flow.

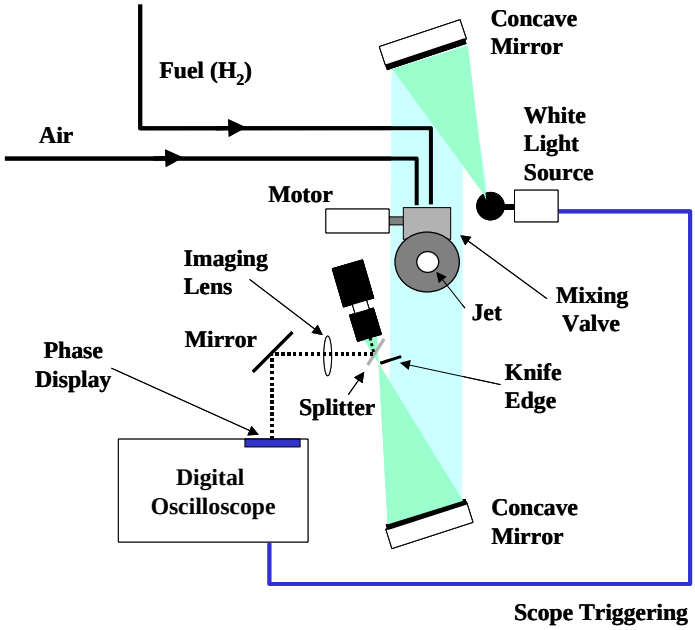

Figure 6: Schlieren Flow Visualization Optical Setup

An image splitter (glass plate) was used to superimpose an image of the phase (trigger time delay) displayed on the triggering oscilloscope and the Schlieren image of the jet flow. This provided a simple and automatic visual recording of the corresponding shaft port orientation during testing.

2.3.2 Image Capture and Triggering

Figures 7(a) and (b) shows the relationship between shaft orientation and trigger delay. Phase-locked images of the exit jet were referenced to the shaft orientation according to the diagram shown in Figure 7(b). The photodetector trigger pulse shown in Figure 7(b) was generated from a photodiode output which sensed HeNe laser light scattered from a piece of retroreflective tape mounted on the rotating shaft. Shaft rotation speeds of up to 45,000 RPM could be achieved with the setup, resulting in porting (pulsation) frequencies of up to 1500 Hz.

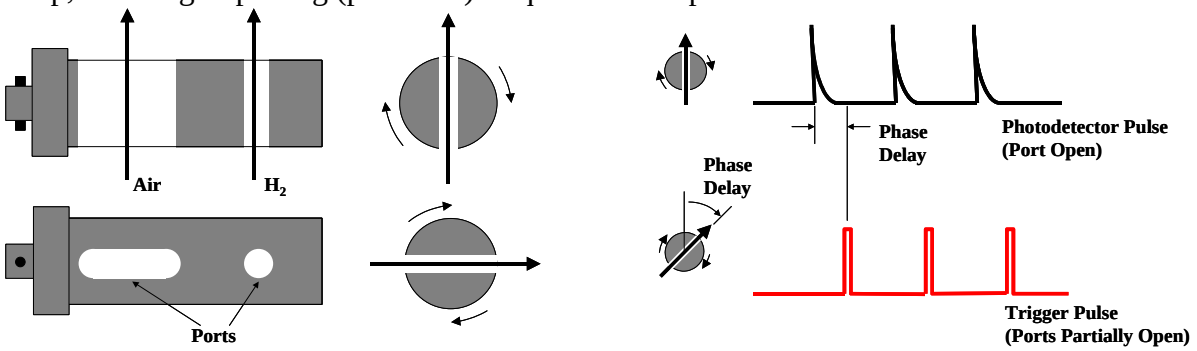

(a) Rotating Shaft Port Orientation **(b) Shaft Phase and Triggering**

Figure 7: Phase and Triggering of Rotating Shaft Porting System

Vertical alignment of the shaft ports and drive pin corresponded to a full open port condition, while horizontal orientation corresponded to a fully closed condition. Any position in between then represented a partially opened condition. It should be noted that this shaft porting system results in two full port openings per revolution. Hence, the porting frequency, f_p , was twice the shaft rotation frequency, f.

3 EXPERIMENTAL RESULTS

Initial testing with airflow was undertaken to demonstrate expected resonant conditions within the range of acoustic frequencies expected for the actuator design. These tests were conducted on the two-section (eight inch long) combustion chamber configuration shown in Figure 2(b). They were expected to reveal lower frequency resonant conditions within the combustion chamber due the lower gas (air) temperatures involved, which would result in significantly lower acoustic wave speeds than those associated with combustion.

3.1 Visualization of Pulsating Air Jet

Schlieren images of the pulsating air jet are shown in Figures 8 for a near resonance condition. The digital display indicates the time delay in milliseconds from a full-open inlet valve position.

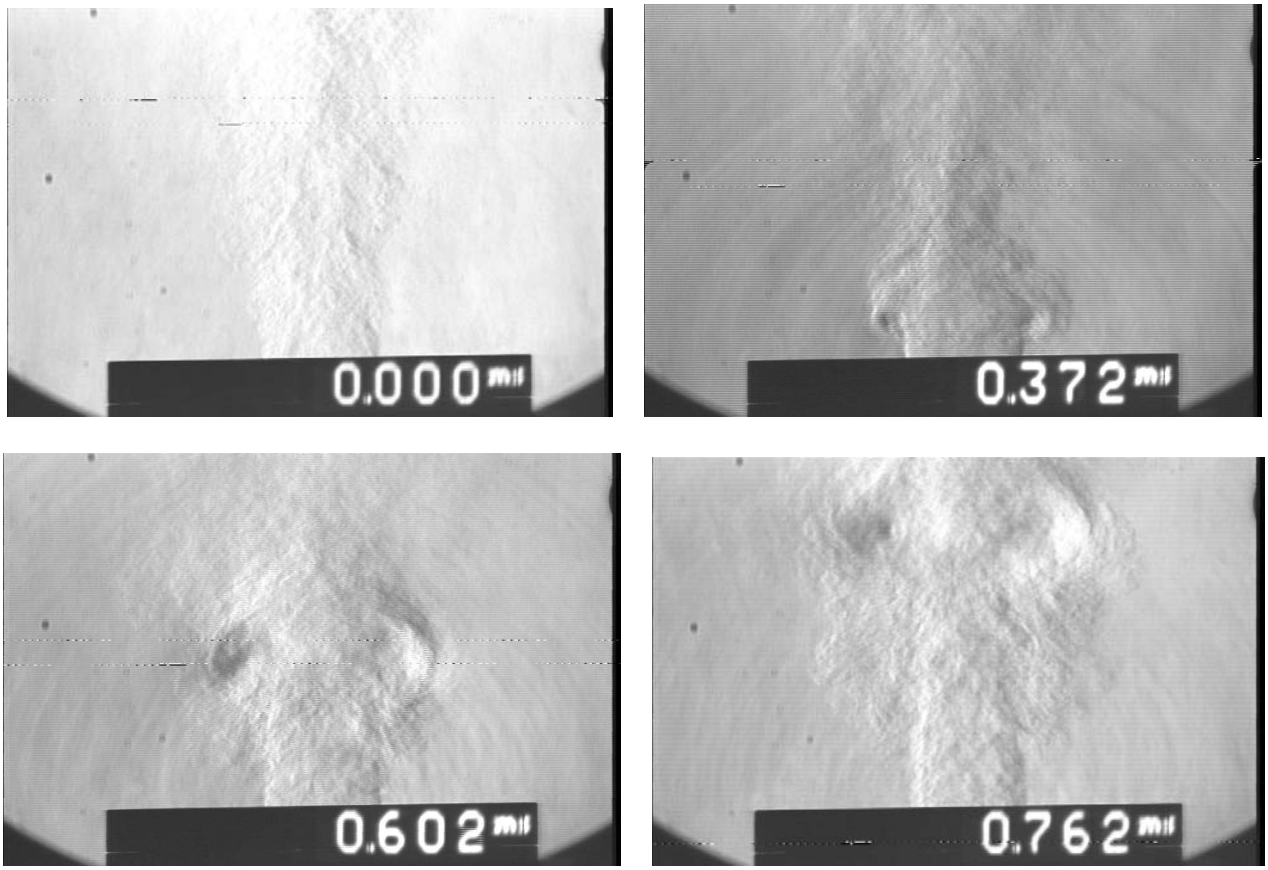

Figure 8: Schlieren Images of Pulsating Jet at Resonance

These near resonance images are for a total inlet airflow of 2408 SLPM @STP, and an average mixing module pressure of 203.8 psig and a temperature of about 70 F. The rotation frequency of the motor shaft was 412 Hz, giving a porting frequency of 824 Hz. It should be noted that the resonance condition for these images was established by simply observing the occurrence of an apparent peak in the pressure oscillation amplitude.

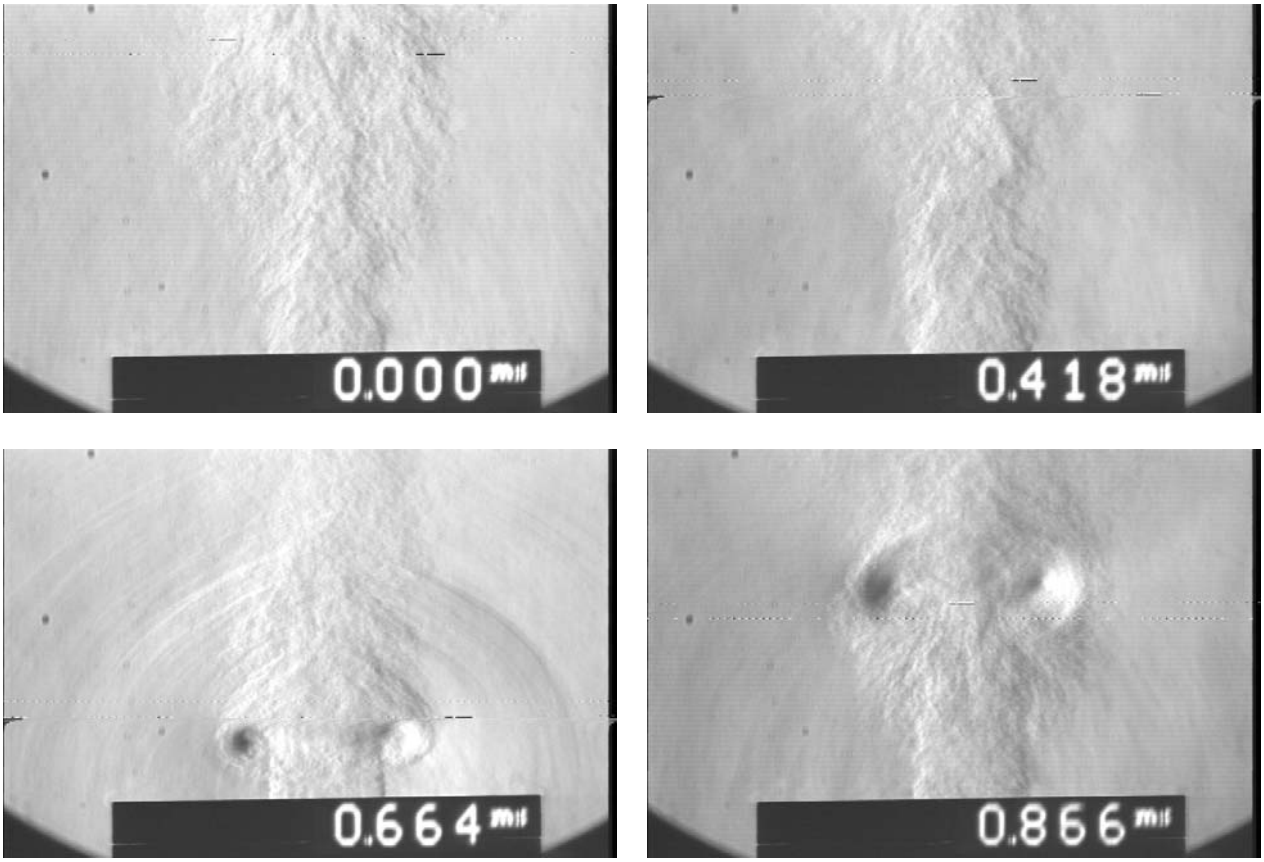

Figure 9: Schlieren Images of Jet Above Resonance

Figure 9 shows a similar set of images for the same two-section chamber configuration, but with a rotation frequency of 472 Hz (944 Hz porting frequency), or slightly above the apparent resonant frequency. The mixing chamber conditions and total airflow were very close those of near resonance. These above resonance images also reveal the growth of an axially symmetric vortex structure, along with the apparent growth of spherically symmetric shock waves emanating from the exit aperture.

3.2 Resonant Pressure Fluctuations

The pressure fluctuation signals from the two pressure taps shown in Figure 2(b) are given in Figure 10. The fundamental oscillation mode resonates in the $\lambda/2$ mode (half wave) in which the pressure distribution at fixed time forms half of a sine wave in the tube, with a node at the center. From Figure 2(b), there is one PCB sensor approximately symmetrically located on each side of this node. Thus, the two pressure sensors will record waveforms that are 180 degrees out of phase from each other.

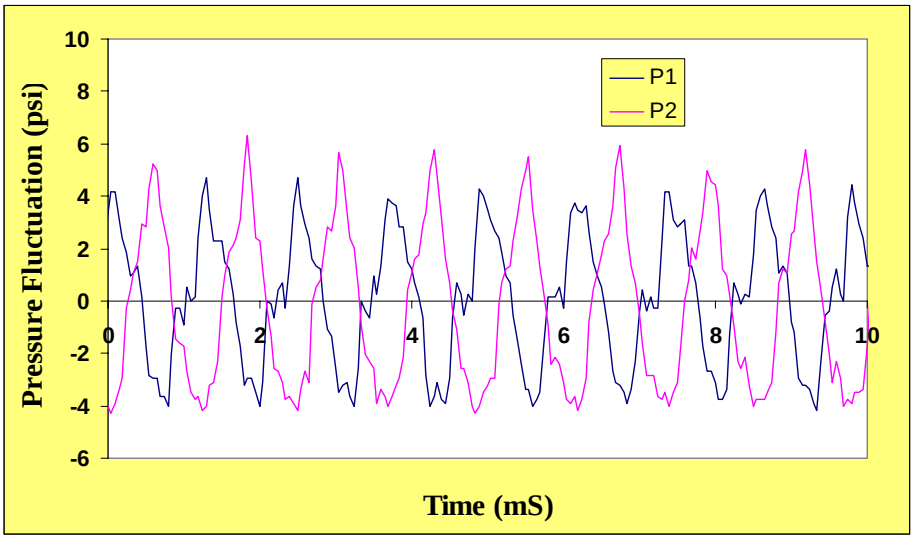

Figure 10: Combustion Chamber Pressure Fluctuations

Figure 11 shows an FFT for the pressure signal associated with the lower pressure tap signal, P_1. The FFT magnitude is plotted over a range of frequencies that includes the fundamental frequency peak of about 821 Hz as well as the next three harmonics in the waveform, which are of much less intensity. This fundamental frequency is very close to the measured porting frequency of $f_p = 2(412 \text{ Hz}) = 824 \text{ Hz}$. From the dominant amplitude of the fundamental peak in Figure 11, it is clear that we are resonating at the fundamental frequency.

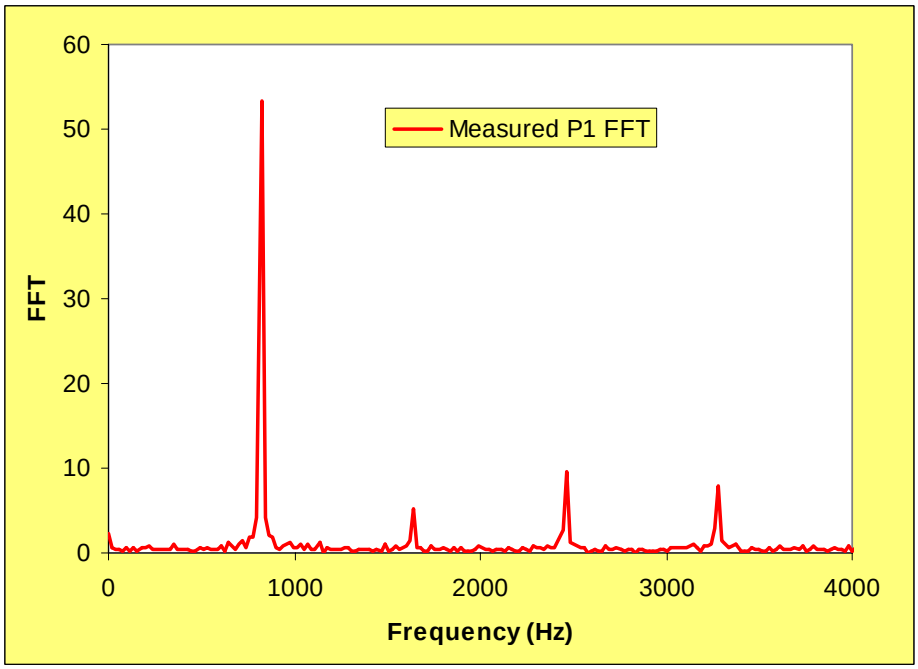

Figure 11: FFT of Measured Pressure Signal, P1

Figure 12 shows that a plot of the successive peak frequencies verses peak number increases linearly, indicating that the peak frequencies are indeed harmonics of the fundamental. The fundamental frequency is consistent with the frequency of an open-ended organ pipe [9] of length L, which is given by

$$f_{pipe} = \frac{c}{2L} \tag{1}$$

where, c is the sound speed given by

$$c = \sqrt{kRT} \tag{2}$$

with k the specific heat ratio, R the gas constant for air, and T is the absolute air temperature. For room temperature atmospheric air at about 70 F, this yields a frequency of about 846 Hz, which is very close to the measured fundamental harmonic frequency of 821 Hz.

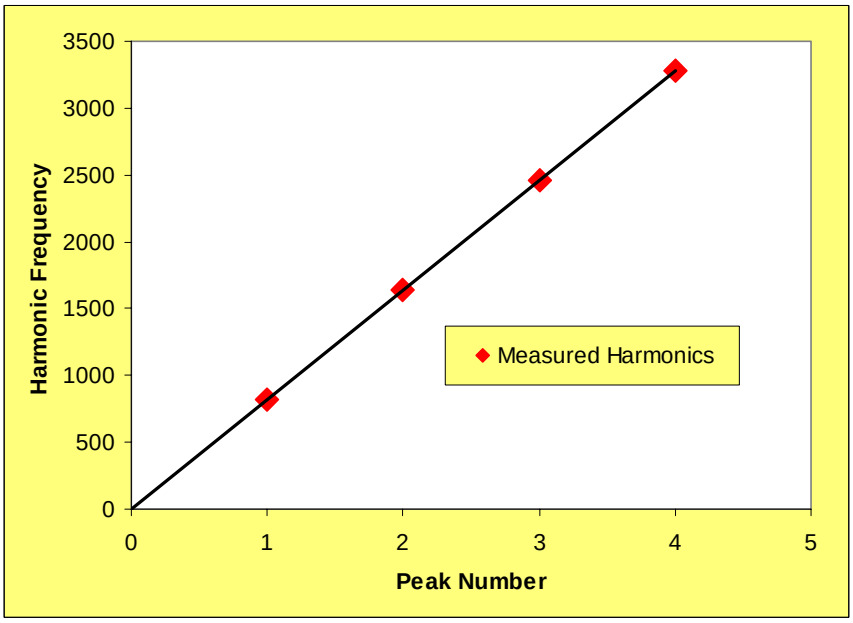

Figure 12: Measured Harmonics of Pressure Fluctuations

3.3 Preliminary Combustion Testing

Preliminary actuator tests with combustion were conducted on a slightly modified version of the setup shown in Figure 2(b). An additional 4.00 inch combustion tube section was inserted in between the two sections shown, and a single PCB pressure sensor was installed in this middle section. The additional section was installed in anticipation of larger acoustic wave propagation speeds in the combustion chamber resulting from the higher gas temperature associated with combustion. Due to the possibility of sensor damage from the extreme internal gas temperatures associated with combustion, and the expected rapid temperature rise once combustion was initiated, only a single pressure tap was used during these initial tests.

3.3.1 Flow Visualization

Combustion was initiated in these first tests by using a propane torch flame igniter directed normal to the axis of the exit jet. The torch was ignited alone at first, followed by the introduction of pure hydrogen gas to produce a large gentle "Bunsen burner" type flame downstream of the jet exit plane, with no apparent combustion inside the cylindrical combustion chamber and no appreciable temperature rise of the externally-mounted thermocouple located near the mixing valve. This initial combustion sequence is shown in Figure 13(a) and 13(b), where the relatively gentle merging of the hydrogen flame and the propane torch flame is observed to take place.

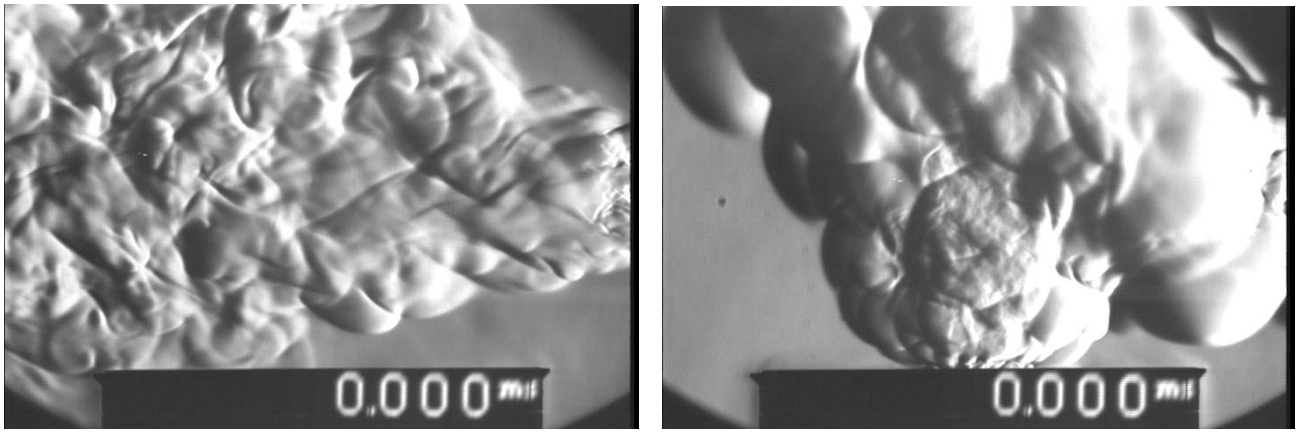

(a) Propane Torch Flame **(b) Ignition of H_2 "Bunsen Burner" Flame**

Figure 13: Initial Combustion Sequence

Airflow was next introduced into the mixing valve and the flame was observed to rapidly "suck" back into the combustion chamber, producing a high speed directed jet at the exit aperture and a very rapid rise in the temperature of the external case-mounted thermocouple. The beginning of the high speed combustion jet is shown in Figure 14(a).

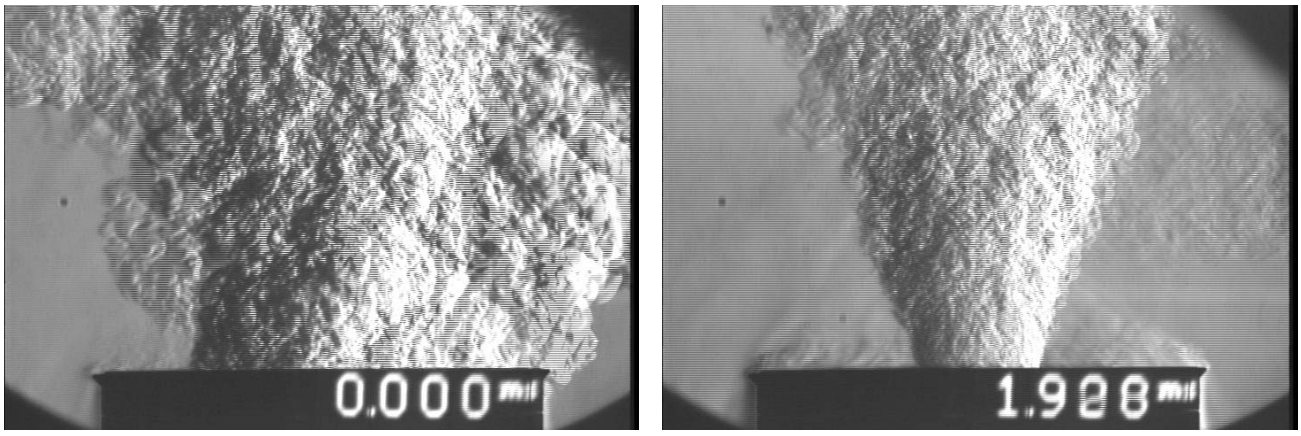

(a) Start of Airflow and Internal Combustion **(b) Established Exit Combustion Jet**

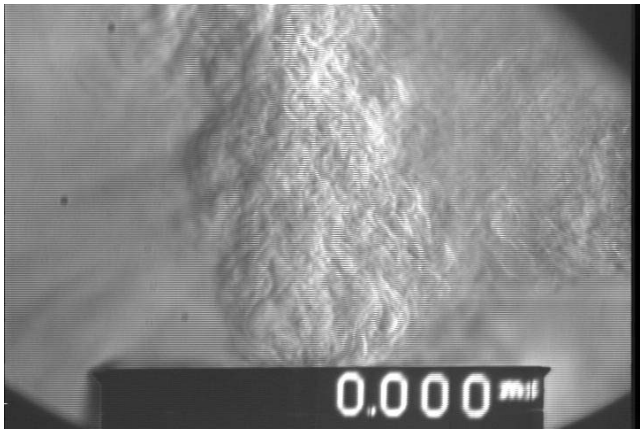

(c) Shutdown and Purge Sequence

Figure 14: Schlieren Images of Preliminary Combustion Tests

The combustion process was only allowed to operate for a few seconds, until the external monitoring thermocouple reached about 200 F. For these initial tests, the flow rate of air was 650 SLPM (air @ STP), the flow rate of hydrogen was 300 SLPM (hydrogen @ STP), and the porting frequency was 800 Hz. Figure 14(b) shows a phase-locked image of the fully established exit jet, and Figure (c) shows an image of the exit plane after the hydrogen flow has been shut down and the air-purging of combustion products has begun. Flameout of the propane torch flame was typically observed shortly after the introduction of airflow, as was the case in Figure 14. Note; however, that the propane gas has not yet been shut down in Figure 14(c) and an unburned and relatively gentle propane gas jet is seen to cross horizontally into the frame from the right.

3.3.2 Sustained Pressure Fluctuations

Sustained pressure oscillations were also observed during these initial combustion tests; however, the amplitude of the oscillations was smaller than observed for the earlier air tests.

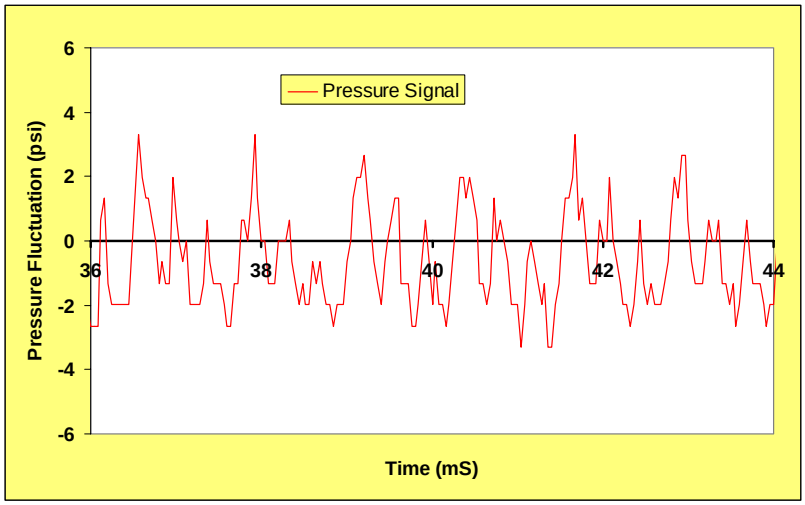

Figure 15: Preliminary Measurements of Pressure Fluctuations with Combustion

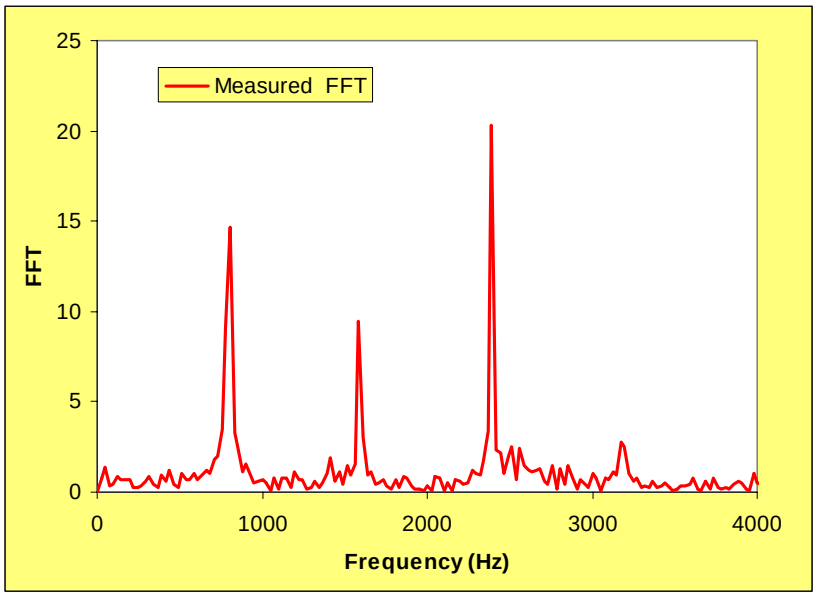

Figure 16: FFT of Pressure Fluctuation for Preliminary Combustion Test

This was due in part to the fact that the mixing valve rotation frequency was considerable below resonance, owing to the increased gas temperature within the combustion chamber. Figure 16 shows the magnitude of the FFT corresponding to the pressure fluctuations shown in Figure 15. It is significant to note that the intensity of the first harmonic is on the same order as that for the fundamental frequency, which corresponds to the porting frequency of 800 Hz. However, the dominant peak is actually at the second harmonic, suggesting that there is a possible resonance condition at much higher frequency than the current porting frequency. This is expected due to the faster acoustic wave speeds encountered with the combustion process.

Additional testing at somewhat higher porting frequencies indicated that, for the given inlet flow rates of hydrogen and air, the maximum porting frequency that would allow sustained combustion was approximately 900 Hz (450 Hz shaft rotation frequency). This work is still in progress and the results presented above represent the state of the experimental research at the end of August 2003.

4 SUMMARY AND CONCLUSIONS

This project involved the experimental testing of a new type of actuator device for potential application to boundary layer control. The device is based on a resonant combustion (and potentially detonation) principle. Initial testing with airflow successfully demonstrated resonant conditions within the range of acoustic frequencies expected for the design. These tests were conducted on a two-section (eight inch long) combustion chamber. Schlieren visualization of the pulsating air jet structure revealed axially symmetric vortex flow, along with the formation of spherically symmetric shocks.

Preliminary testing with combustion was also undertaken using a slightly modified version of the same design consisting of a three-section (12-inch long) combustion chamber test section. These tests, which successfully demonstrated sustained combustion of hydrogen along with sustained pressure oscillations, suggest that resonance will occur at a much higher frequency than was excited

by the pulsating fuel injection in the current test as would be expected with the much higher combustion temperatures. This work is still in progress and demonstration of operation of the actuator in resonant mode will be reported in future papers.

ACKNOWLEDGEMENTS

The authors would like to thank the NASA Langley Research Center for their support of this research. This work was conducted under an ASEE NASA Faculty Fellowship Summer 2003 Program appointment. The authors would also like to acknowledge the coordination efforts of Dr. Paul Danehy in helping to make this appointment possible. The assistance of Mr. Fred Rudolph, Technician, and Mr. Carlos Cartillo, Machinist, are also much appreciated. In addition, the authors would like to acknowledge the many suggestions, discussions, and valuable technical assistance of NRC Associate Dr. Sean O'Byrne during this phase of the research.

REFERENCES

1. Funk, R., Parekh, D., Crittenden, T. and Glezer, A., Transient Separation Control using Pulse Combustion Actuation, 1st Flow Control conference, 24-26 June 2002, Paper# AIAA 2002-3166.
2. NASA Langley Research Center, Fact Sheet# FS-2000-06-52-LaRC.
3. McCormick, B. W., *Aerodynamics, Aeronautics and Flight Mechanics*, 2nd Edition, Wiley, pp. 86-109, 1995.
4. Grossman, K. R., Cybyk, B. Z., and VanWie, D. M., Sparkjet Actuators for Flow Control, 41st AIAA Aerospace Sciences Meeting & Exhibit, 6-9 June 2003, Paper# AIAA-2003-0057.
5. Crittenden, T. and Glezer, A., Funk, R., Parekh, D., Combustion-Driven Jet Actuators for Flow Control, 31st AIAA Fluid Dynamics Conference & Exhibit, 11-14 June 2001, Paper# AIAA 2001-2768.
6. Rinehart, C., McMichael, J. M., and Glezer, A., Transitory Flow and force Development on a Body of Revolution Using Synthetic Jet Actuation, Paper# AIAA 2003-0618.
7. Kuo, K. K., *Principles of Combustion*, Wiley, 1986, pp. 231-283.
8. Settles, G. S., Schlieren and Shadowgraph Techniques, Springer, pp. 42-44, 1949.
9. Resnick, R., and Halliday, D., *Physics*, Part I, John Wiley & Sons, pp. 497-512, 1966.